



GAIN-SCHEDULED SEISMIC ISOLATION CONTROL CONSIDERING ACTUATOR SATURATION FOR BUILDING-LIKE STRUCTURES

Noriaki ITAGAKI¹ and Hidekazu NISHIMURA²

SUMMARY

In this paper we propose a design method for active seismic isolation control taking account of actuator saturation. By using a hyperbolic tangential function that is differentiable to controller output, we formulate the linear parameter varying system according to the controller output and design a gain-scheduled controller. By carrying out simulations and experiments of seismic excitation, our proposed gain-scheduled controller is compared with an H_∞ fixed controller or a sliding mode controller. It is verified that the proposed controller maintains performance of isolation even if a large earthquake with which the actuator saturation occurs comes, although the other controllers lower the performance than uncontrolled case.

INTRODUCTION

Seismic isolation techniques have attracted Japanese citizen's attention as the technique for the structural design of building-like structures after Hanshin-Awaji earthquake. While not only passive vibration isolation equipments using passive dampers but also a semi-active vibration isolation equipment (Santo and Yoshida, 2002) have been practical use (Yoshida, 2001), active vibration isolation control methods (Nishimura and Kojima, 1998, Nishimura and Kojima 1999) have been studied.

The control system designed by using an ordinary linear control method such as Linear Quadratic Gaussian or H_∞ control theory may lower the performance if input saturation occurs. In order to overcome this saturation problem many researchers have studied. Jabbari and Kim have proposed a technique that reduces the computational burden of the linear matrix inequalities (LMIs) for the cases where several actuators are used, and have applied it to the issue of the actuator saturation for a six story building. It has been shown that although the relative displacement between the base and the first story

¹ Graduate School of Science and Technology, Chiba University, Chiba, Japan. Email: puri@graduate.chiba-u.jp

² Faculty of Engineering, Chiba University, Chiba, Japan. Email: nism@faculty.chiba-u.jp

was suppressed, the first story acceleration became the same response as uncontrolled case (Kim and Jabbari, 2002, Nguyen, Jabbari and Miguel, 1998). Santo, Watanabe and Yoshida have shown the design method of a sliding mode (SM) controller for the active vibration isolation system. They have proposed the method of the gain adjustment between the linear control and the nonlinear control in order to overcome the actuator saturation (Santo, Watanabe and Yoshida, 1999, 2000). We have already proposed the design method of a gain-scheduled (GS) control system considering the actuator constraint by using a hyperbolic tangential function as a saturation function (Nishimura and Oie, 2000, Nishimura and Shimodaira, 2002). The differentiable function has advantage from the viewpoint of less excitation of vibration modes than the undifferentiable function such as a saturated function, when the control input is saturated.

In this paper we introduce scheduling of an active vibration isolation controller based on the reference (Nishimura and Shimodaira, 2002). By formulating the input saturation as a hyperbolic tangential function we obtain the linear parameter varying (LPV) system according to the control input that the controller needs. The GS controller is designed using the LMIs (Gahinet, Nemirovski, Laub and Chilali, 1995) so that the nominal performance of suppression on acceleration response is held against larger earthquakes as much as possible. The controller uses acceleration of the lowest story only as a feedback signal and is implemented to the experimental setup of a four-degree-of-freedom structure. A voice-coil motor is used as an actuator and the limitation of the actuator is given. Real-time discretization of the controller is realized by Padé approximation in every sampling time (Takagi and Nishimura, 1999, Itagaki and Nishimura, 2002). Five representative earthquakes data are used by adjusting their amplitude for our experimental setup. By carrying out simulations and experiments it is verified that performance of the proposed GS controller is superior in comparison with an H_∞ fixed controller or an SM controller.

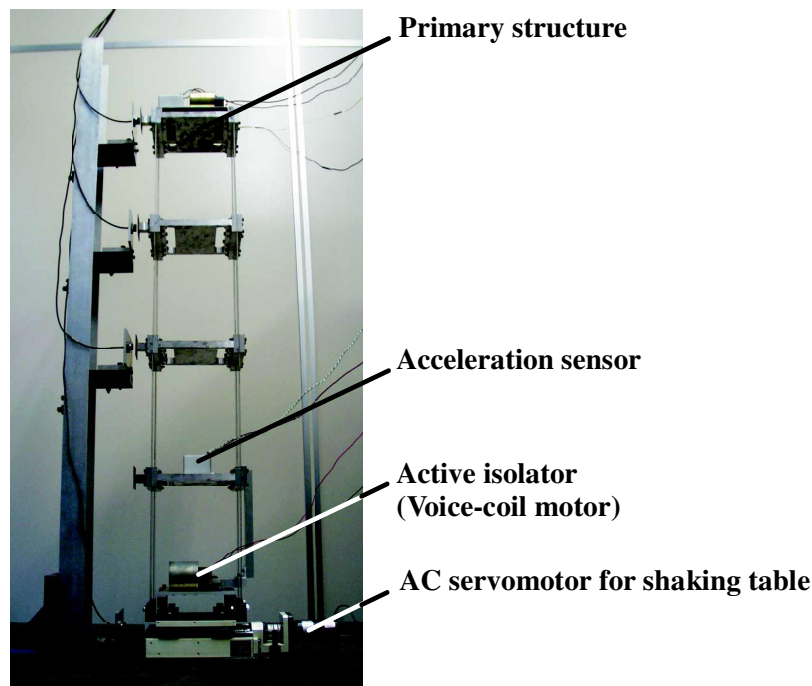


Fig. 1 Experimental setup

MODELLING OF CONTROLLED STRUCTURE

Figure 1 shows a four-degree-of-freedom structure with an active vibration isolation device used as an experimental setup in our laboratory. An acceleration sensor is put on the lowest story for a feedback signal. The active isolator is installed in isolation layer and consists of a voice-coil motor, a linear slide bearing and a connecting rod. The primary structure is put on the shaking table that can be driven by an AC servomotor. Figure 2 shows a dynamical model of Fig. 1. Table 1 shows specifications of the dynamical model.

In this study we assume that thrust of the voice-coil motor has saturation at a constant value of $|\alpha| = 0.5$ N. We describe the limitation of the input to the system by the following hyperbolic tangential function of the controller output u :

$$u_s = \alpha \tanh\left(\frac{u}{\alpha}\right). \quad (1)$$

The hyperbolic tangential function as a saturation function is indicated by the solid line in Fig. 3 (a). Using the state vector:

$$x_f = [x_s^T \dot{x}_s^T]^T \quad \text{where} \quad x_s = [x_1 \ x_2 \ x_3 \ x_4]^T,$$

we have the following state equation of the full-order model neglecting the actuator constraint:

$$\dot{x}_f = A_f x_f + B_{fz} \ddot{z} + B_{fu} u_s. \quad (2)$$

Both the first story acceleration of the primary structure $\ddot{x}_1 + \ddot{z}$ and the relative displacement $x_2 - x_1$ between the first story and the second story are controlled output and the output equation is

$$y_f = \begin{bmatrix} \ddot{x}_1 + \ddot{z} \\ x_2 - x_1 \end{bmatrix} = C_f x_f + D_{fu} u_s. \quad (3)$$

Furthermore, by using the balanced realization method the following reduced-order model for the controller design is obtained truncating the third and the fourth modes from Eq. (2), (3)

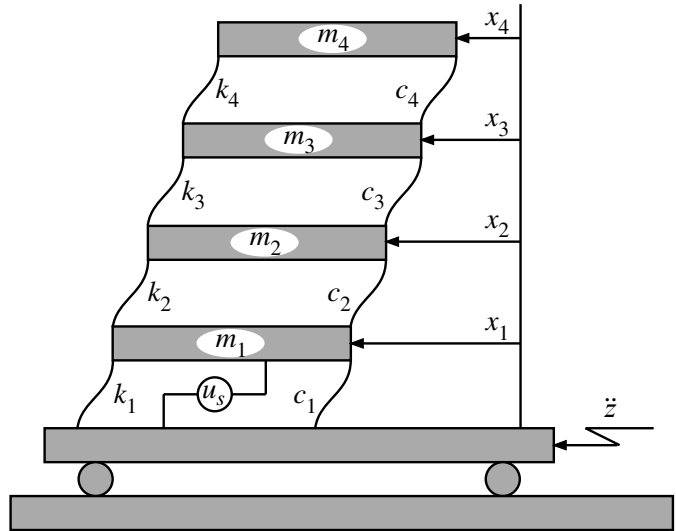
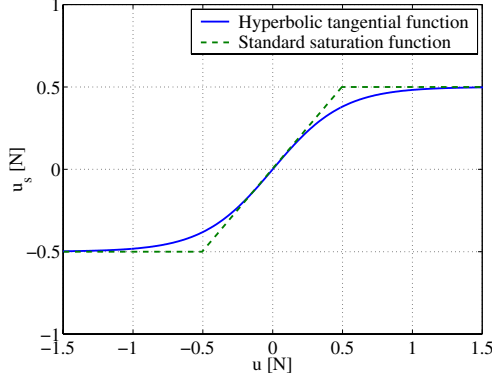


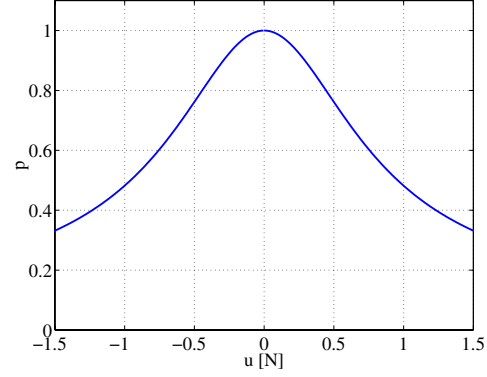
Fig. 2 Dynamical model of controlled object

Table 1 Parameters of experimental setup

Parameter		Value
Mass	m_1	1.61 kg
	m_2	1.38 kg
	m_3	1.38 kg
	m_4	1.30 kg
Spring	k_1	2050 N/m
	k_2	2250 N/m
	$k_i (i = 3, 4)$	2550 N/m
Damping	c_1	3.278 Ns/m
	c_2	0.278 Ns/m
	c_i	0.078 Ns/m



(a) Saturation function



(b) Scheduling parameter p

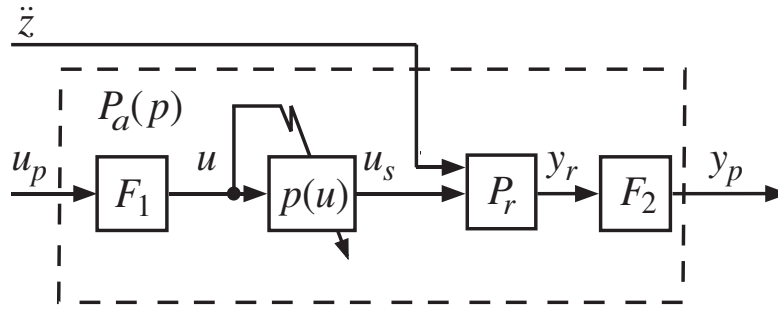


Fig. 4 Structure of LPV system $P_a(p)$

$$\begin{aligned} \dot{x}_r &= A_r x_r + B_{rz} \ddot{z} + B_{ru} u_s, \\ y_r &= C_r x_r + D_{rz} \ddot{z} + D_{ru} u_s. \end{aligned} \quad (4)$$

The state equation including Eq. (1) can be rewritten as follows:

$$\begin{aligned} \dot{x}_r &= A_r x_r + B_{rz} \ddot{z} + B_{ru} (p(u))u, \\ y_r &= C_r x_r + D_{rz} \ddot{z} + D_{ru} (p(u))u, \end{aligned} \quad (5)$$

$$p(u) = (\alpha \tanh(u/\alpha))/u. \quad (6)$$

It is worth noting that B_{ru} and D_{ru} in the LPV system obtained change in accordance with the scheduling parameter $p(u)$ as shown in Fig. 3 (b).

Since the LMIs based GS control (Gahinet, Nemirovski, Laub and Chilali, 1995) requires the condition that the elements of the control input matrix are constant and the elements of the transfer matrix are zero, we respectively add the low-pass filters $F_1(s)$ and $F_2(s)$ to the input of the plant and the output of the plant, as shown in Fig. 4. The low-pass filters $F_1(s)$ and $F_2(s)$ are chosen as follows:

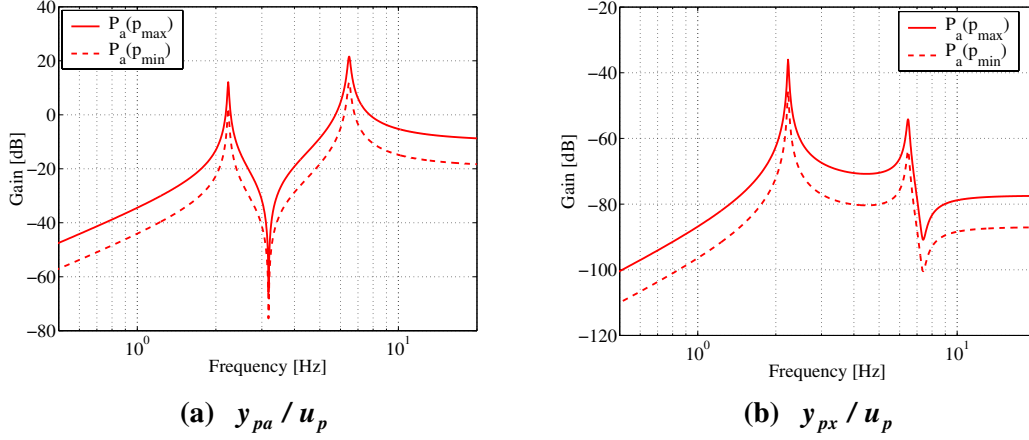


Fig. 6 Generalized plant $G_{zw}(p)$

$$F_1(s) = L_p(s), \quad F_2(s) = \text{diag}(L_p(s), L_p(s)), \quad L_p(s) = \frac{1}{as + 1}, \quad a = 10^{-3}. \quad (7)$$

The augmented system $P_a(p)$ is obtained as follows:

$$\begin{aligned} \dot{x} &= A(p)x + B_r \ddot{z} + B_u u_p, \\ y_p &= \begin{bmatrix} y_{pa} & y_{px} \end{bmatrix}^T = Cx + D_{rz} \ddot{z}. \end{aligned} \quad (8)$$

Furthermore, $A(p)$ can be described as an affine dependence on scheduling parameter p . Equation (8) can be formulated as follows:

$$\dot{x} = (A_0 + pA_p)x + B_r \ddot{z} + B_u u_p. \quad (9)$$

Thus, we can obtain the linear time-invariant (LTI) controllers that correspond to the vertexes of the parameter box. The GS controller $K(p)$ corresponding to a point in the box is given as the convex interpolation of the vertex LTI controllers. We restrain the controller output u in the range from -1.5 to 1.5 N, and the scheduling parameter p varies in the range $p \in [\tanh(3)/3, 1]$. The gain diagram of y_{pa}/u_p and y_{px}/u_p are shown in Figs. 5 (a) and (b), respectively.

DESIGN OF GAIN-SCHEDULED CONTROLLER

By applying the LMIs based GS control (Gahinet, Nemirovski, Laub and Chilali, 1995), we design the controller for the LPV system $P_a(p)$ obtained so as to guarantee that the H_∞ norm of G_{zw} is less than a certain value as follows:

$$\|G_{zw}\|_\infty < \gamma, \quad (10)$$

where

$$\begin{bmatrix} z_1 & z_{21} & z_{22} \end{bmatrix}^T = G_{zw} \begin{bmatrix} w_1 & w_2 \end{bmatrix}^T. \quad (11)$$

The generalized plant for controller design is shown in Fig. 6, where w_1 is the disturbance input \ddot{z} , y_{pa} is the observed variables, and z_1 , z_{21} and z_{22} are the controlled variables. The additive perturbation Δ_d is considered through the transfer function from w_2 to z_1 by the weighting function W_T . In order to isolate vibration from the base, we set not only the weighting function W_{s1} for the first story acceleration $\ddot{x}_1 + \ddot{z}$ but also W_{s2} for the relative displacement $x_2 - x_1 (= y_{px})$ between the first story and the second story (Nishimura and Kojima, 1998). W_N is the parameter for the observation noise. The gain diagram of the additive error and the weighting functions is shown in Fig. 7.

The obtained LTI vertex controllers $K(p_{\max})$ and $K(p_{\min})$ are shown in Fig. 8. $K(p_{\max})$ and $K(p_{\min})$ is respectively corresponding to the maximum value p_{\max} and the minimum value p_{\min} of the scheduling parameter p . Also, the frequency band of the low-pass filters $F_1(s)$ and $F_2(s)$ used to formulate the LPV system $P_a(p)$ is sufficiently wide that we have removed $F_1(s)$ and $F_2(s)$. Figure 9 shows the frequency response function $(\ddot{x}_1 + \ddot{z})/\ddot{z}$ of the closed-loop system using LTI vertex controllers $K(p_{\max})$ and $K(p_{\min})$.

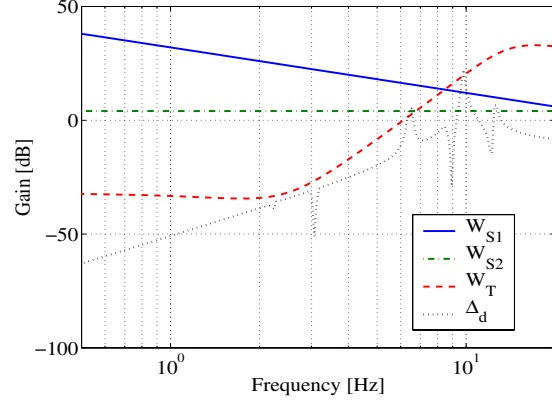


Fig. 7 Gain diagram of additive error and weighting functions

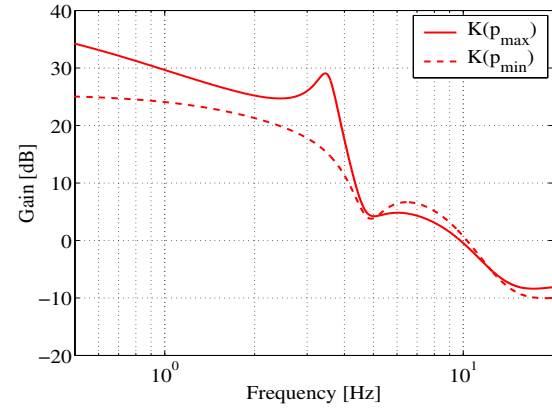


Fig. 8 Gain diagram of LTI vertex controllers $K(p_{\max})$ and $K(p_{\min})$

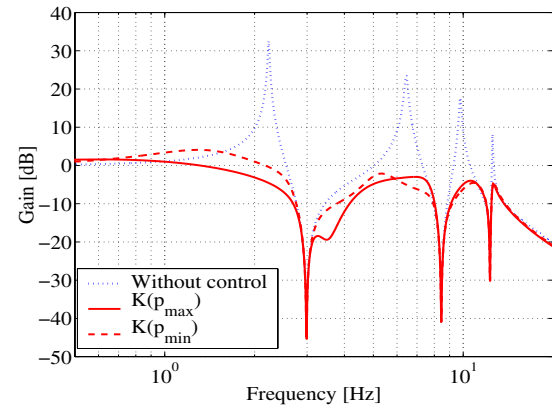


Fig. 9 Frequency responses of closed-loop system using LTI vertex controllers $K(p_{\max})$ and $K(p_{\min})$

Figure 9 shows the frequency response function $(\ddot{x}_1 + \ddot{z})/\ddot{z}$ of the closed-loop system using LTI vertex controllers $K(p_{\max})$ and $K(p_{\min})$.

From Figs. 8 and 9 we can see that the vertex controller $K(p_{\max})$ intends to mainly suppress the first mode vibration. On the contrary, the vertex controller $K(p_{\min})$ increases the gain of the frequency response in the frequency range of the second mode and decreases that of the first mode. The GS controller is given by convex interpolation as follows:

$$K(p) = \frac{p_{\max} - p}{p_{\max} - p_{\min}} K(p_{\min}) + \frac{p - p_{\min}}{p_{\max} - p_{\min}} K(p_{\max}). \quad (12)$$

This controller varies in accordance with the scheduling parameter p . Real-time discretization of the GS controller is realized by Padé approximation in every sampling time of 2ms (Takagi and Nishimura, 1999, Itagaki and Nishimura, 2002).

For both the H_{∞} fixed controller and the SM controller, the input to the system assumed to be constrained by using the standard saturation function indicated by the broken line in Fig. 3 (a). The H_{∞} fixed controller is designed for the reduced model of Eq. (4). The SM controller is designed for the full-order model of Eq. (2), (3) because it is difficult to take spillover phenomena due to truncated modes into account. The state variables used as feedback signals of the SM controller are estimated by a Kalman filter.

RESULTS OF SIMULATION AND EXPERIMENT

Responses to Level 1 earthquake

We assume Level 1 earthquake whose amplitude is adjusted so that the actuator saturation does not occur. Figures 10 (a) and (b) respectively show the first story acceleration response $\ddot{x}_1 + \ddot{z}$ and the control input u_s of the GS controller to Level 1 seismic wave of the Hanshin-Awaji earthquake. The solid lines and the broken lines indicate the responses of the experimental results and those of the simulation results, respectively. It is seen that the experimental results are good agreement with the simulation results.

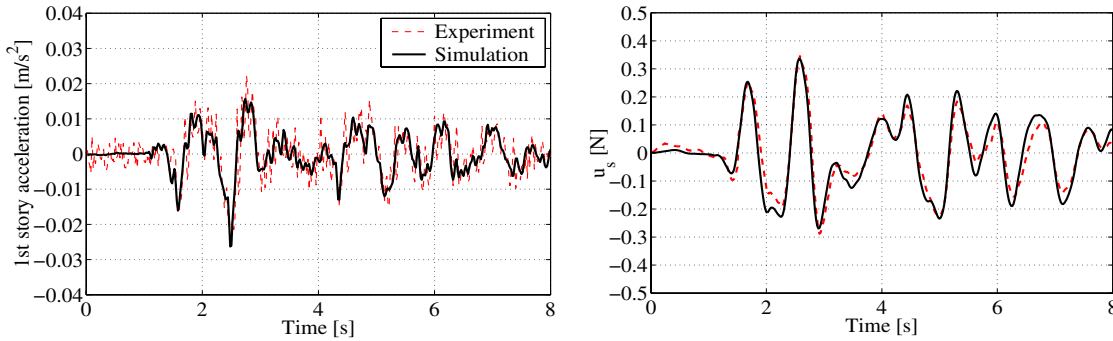


Table 2 Amplitude multiplier (Level 1)

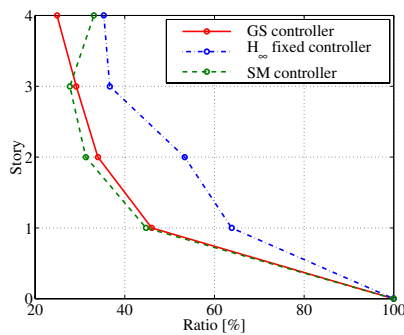
Hanshin-Awaji	Hachinohe	Taft	El Centro	Northridge
2.35×10^{-3}	9.0×10^{-3}	1.68×10^{-2}	8.64×10^{-3}	7.0×10^{-3}

Table 3 Ratio of 1st story acceleration r.m.s. value against earthquake (Level 1) [%]

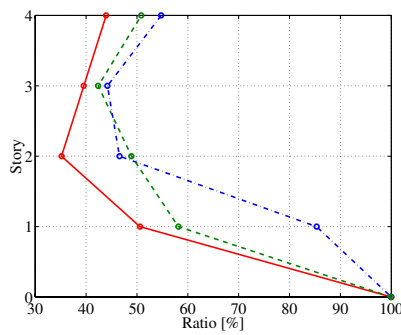
	Hanshin-Awaji	Hachinohe	Taft	El Centro	Northridge
GS controller	17.19	25.77	14.45	18.11	26.94
H_∞ fixed controller	18.69	26.95	14.34	18.47	24.69
SM controller	16.97	25.46	14.39	17.23	27.02
Without control (mm/s^2)	100.0 (32.67)	100.0 (16.01)	100.0 (43.76)	100.0 (35.22)	100.0 (25.50)

Table 4 Ratio of 4th story acceleration r.m.s. value against earthquake (Level 1) [%]

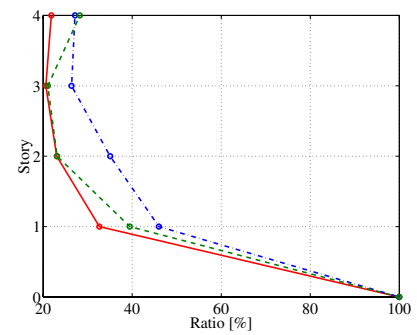
	Hanshin-Awaji	Hachinohe	Taft	El Centro	Northridge
GS controller	15.58	25.46	13.20	13.74	28.62
H_∞ fixed controller	15.80	23.17	12.79	13.71	26.99
SM controller	15.22	23.37	12.38	12.81	28.40
Without control (mm/s^2)	100.0 (75.91)	100.0 (37.56)	100.0 (105.6)	100.0 (82.00)	100.0 (53.97)



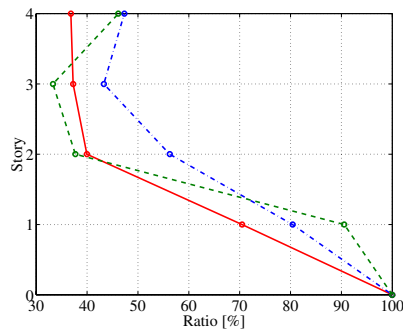
(a) Hanshin-Awaji earthquake



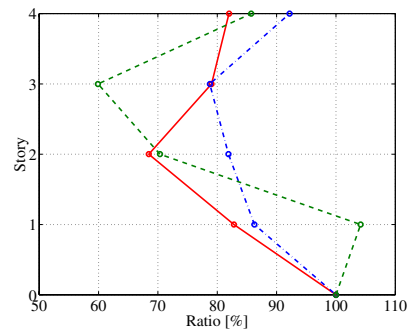
(b) Hachinohe earthquake



(c) Taft earthquake

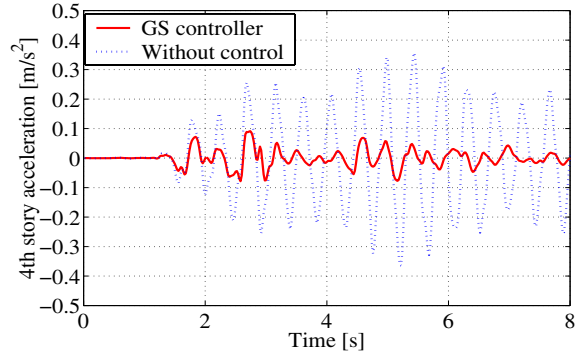


(d) El Centro earthquake

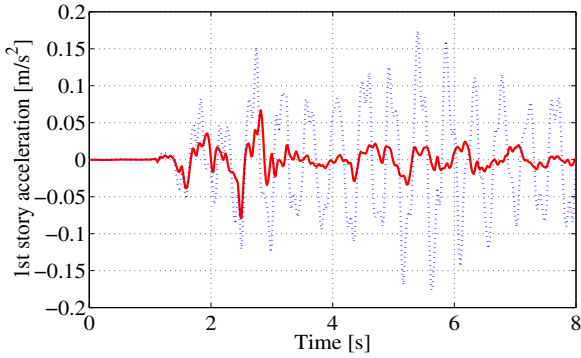


(e) Northridge earthquake

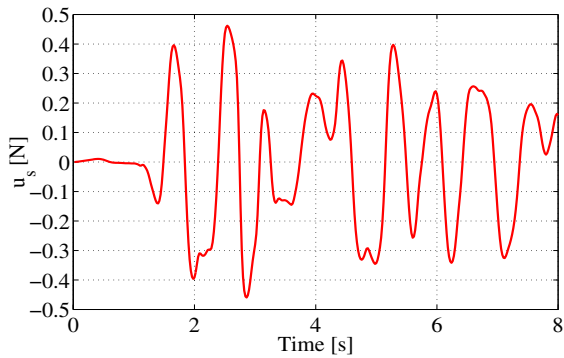
Fig. 11 Ratio of maximum accelerations against earthquake (Level 2-1)



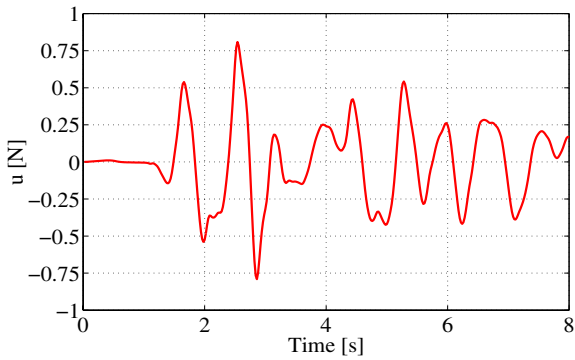
(a) $\ddot{x}_4 + \ddot{z}$



(b) $\ddot{x}_1 + \ddot{z}$

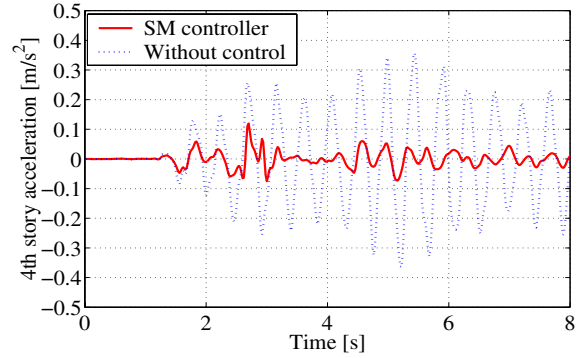


(c) u_s

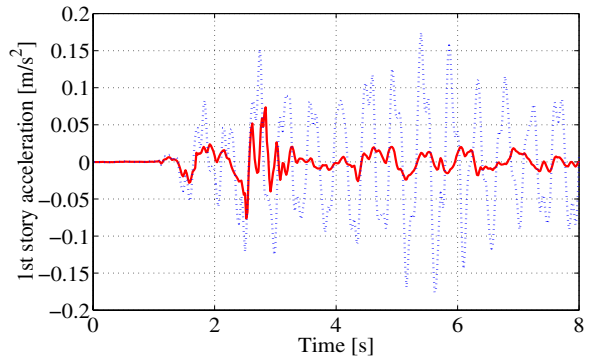


(d) u

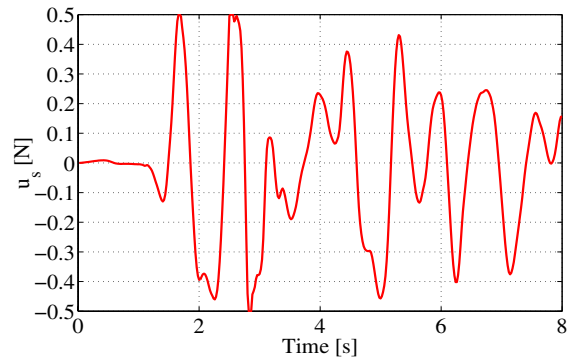
Fig. 12 Time history responses against Hanshin-Awaji earthquake (Level 2-1) by GS controller



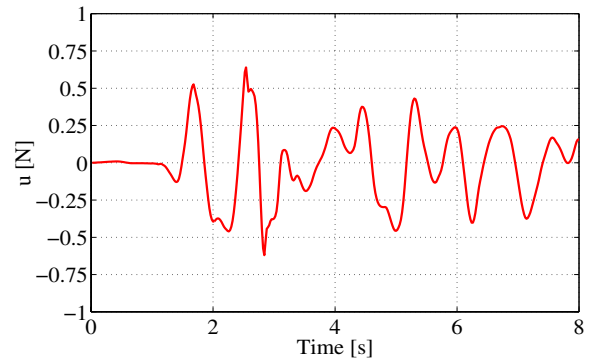
(a) $\ddot{x}_4 + \ddot{z}$



(b) $\ddot{x}_1 + \ddot{z}$



(c) u_s



(d) u

Fig. 13 Time history responses against Hanshin-Awaji earthquake (Level 2-1) by SM controller

Table 2 shows the amplitude multiplier that is multiplied by the actual earthquake data in Level 1 earthquake case. Table 3 and 4 respectively show the ratio of the root mean square (r.m.s.) value of the first story acceleration and the fourth story acceleration with control to that without control obtained in simulation results. The GS controller hardly varies because the change of the scheduling parameter p is very small in Level 1 earthquake case. The GS controller, the H_∞ fixed controller and the SM controller are designed so as to have the same performance.

Responses to Level 2 earthquake

We assume Level 2-1 earthquake whose amplitude is multiplied by 2.0 for Level 1 earthquake. Figures 11 (a), (b), (c), (d) and (e) respectively show the ratio of the maximum acceleration against Level 2-1 earthquake to that without control obtained in simulation results. The solid lines, the dash-dotted lines and the broken lines indicate the GS controller, the H_∞ fixed controller and the SM controller, respectively. It is seen from Fig. 11 that the GS controller maintains the good control performance, while the H_∞ fixed controller lowers the control performance. From Figs. 11 (a), (b) and (c), we can see that both the GS controller and the SM controller have same good performance. Since the SM controller has robustness due to satisfaction of matching condition (Santo, Watanabe and Yoshida, 1999, 2000), the SM controller hardly saturates. In case of El Centro earthquake and Northridge earthquake, however, the first story acceleration of the SM controller becomes worse than that of the H_∞ fixed controller as shown in Figs. 11 (d) and (e).

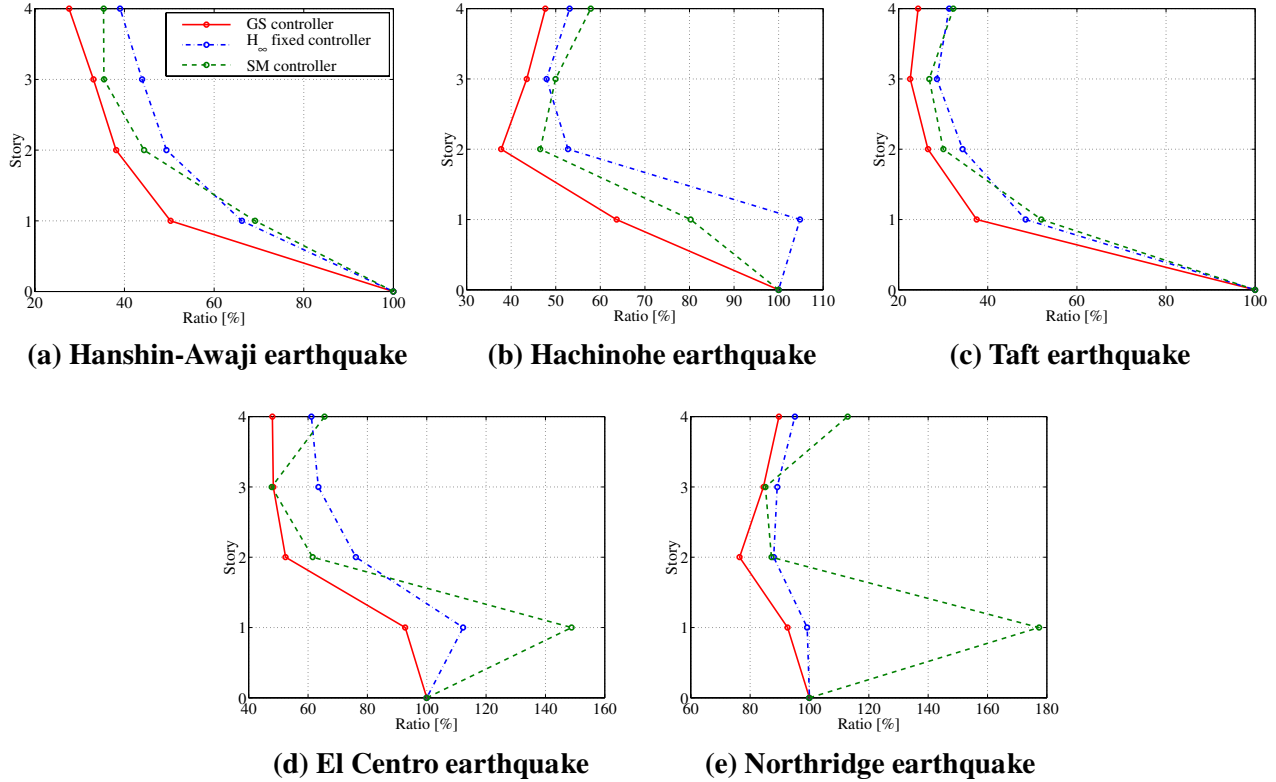


Figure 12 and 13 respectively show the simulation results of the GS controller and the SM controller against Hanshin-Awaji earthquake of Level 2-1. Figures 12, 13 (a), (b), (c) and (d) respectively show the fourth story acceleration $\ddot{x}_4 + \ddot{z}$, the first story acceleration $\ddot{x}_1 + \ddot{z}$, the control input u_s and the controller output u . It is seen from Figs. 12, 13 (a) and (b) that both the GS controller and the SM controller have the same good performance against the Hanshin-Awaji earthquake of Level 2-1. Since the GS controller uses the hyperbolic tangential function as the saturation function, the control input is smaller than the limitation $\pm 0.5 \text{ N}$ as shown in Fig. 12 (c) even when the controller output exceeds the limitation as shown in (d). As the control input becomes near the limitation $\pm 0.5 \text{ N}$, the scheduling parameter p reduces, and the GS controller varies according to the scheduling parameter p as shown in Fig. 8 and Eq. (12). On the contrary, the control input of the SM controller whose gain between the linear control and the nonlinear control is appropriately adjusted hardly saturates as shown in Figs. 12 (c) and (d) (Santo, Watanabe and Yoshida, 1999, 2000).

We assume Level 2-2 earthquake whose amplitude is multiplied by 2.5 for Level 1 earthquake. Figures 14 (a), (b), (c), (d) and (e) respectively show the ratio of the maximum accelerations against Level 2-2 earthquake to that without control obtained in simulation results. The solid lines, the dash-dotted lines and the broken lines indicate the GS controller, the H_∞ fixed controller and the SM controller, respectively. It is seen that the GS controller proposed maintains performance of vibration isolation against even the Level 2-2 earthquake as shown in Figs. 14 (a) to (e). In case of Hachinohe earthquake and El Centro earthquake, the maximum value of the first story acceleration by the H_∞ fixed controller becomes worse than that without control as shown in Figs. 14 (b) and (d). In case of El Centro earthquake and Northridge earthquake,

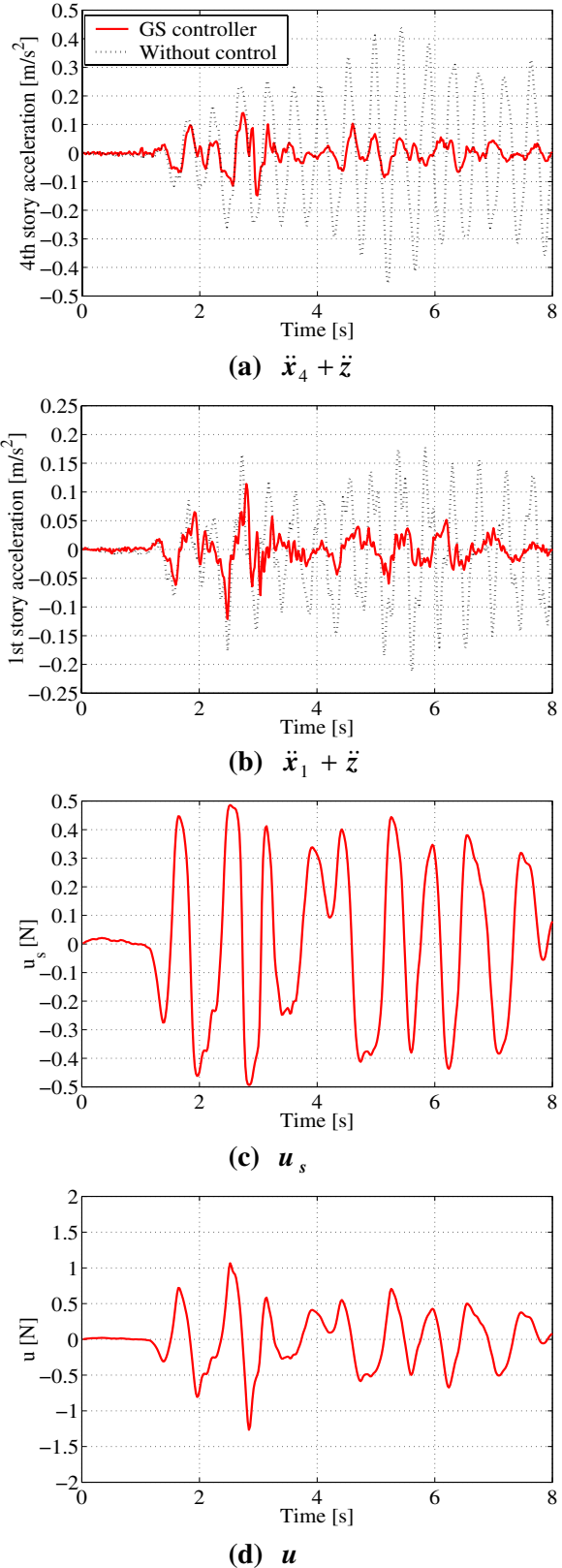
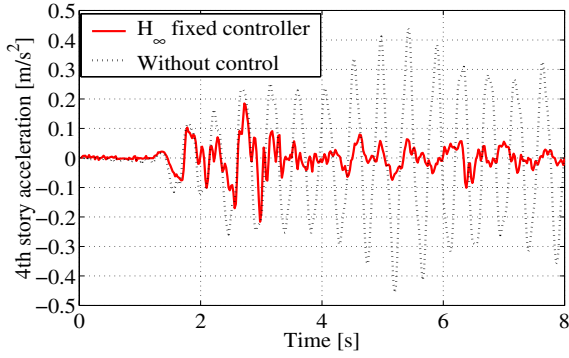
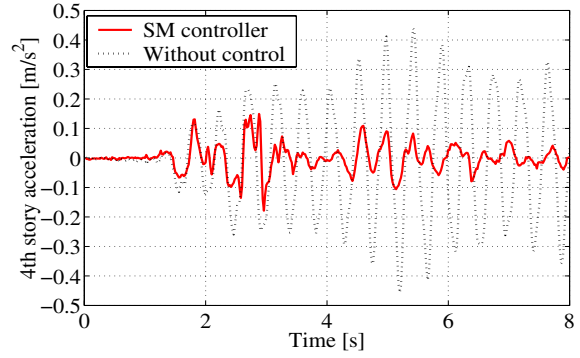


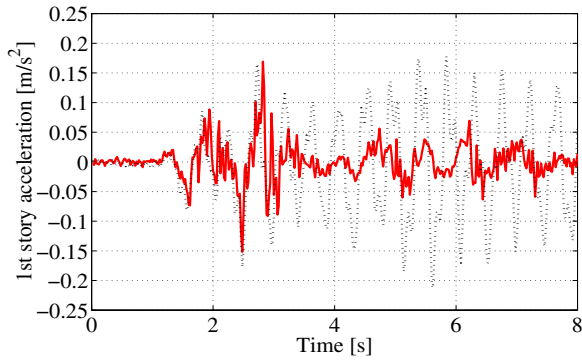
Fig. 15 Time history responses against Hanshin-Awaji earthquake (Level 2-2) by GS controller



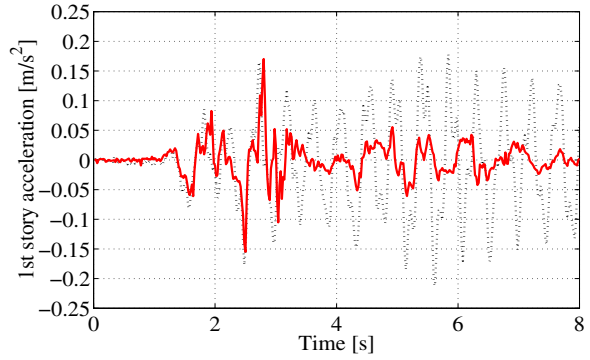
(a) $\ddot{\mathbf{x}}_4 + \ddot{\mathbf{z}}$



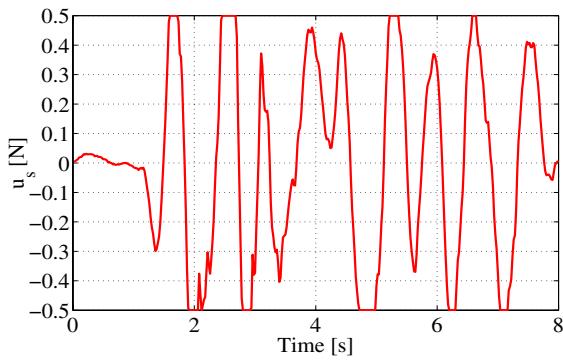
(a) $\ddot{\mathbf{x}}_4 + \ddot{\mathbf{z}}$



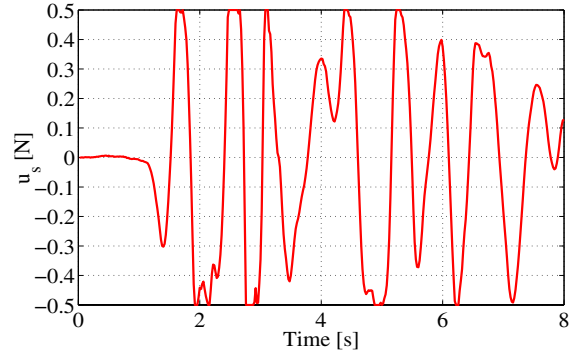
(b) $\ddot{\mathbf{x}}_1 + \ddot{\mathbf{z}}$



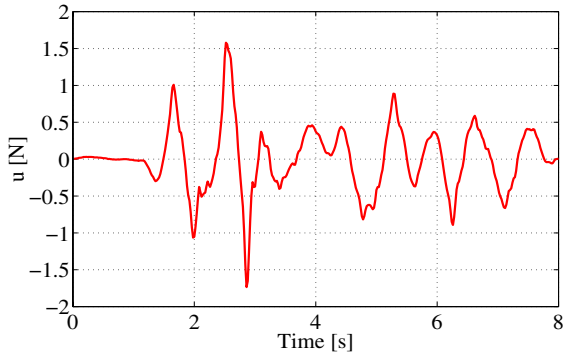
(b) $\ddot{\mathbf{x}}_1 + \ddot{\mathbf{z}}$



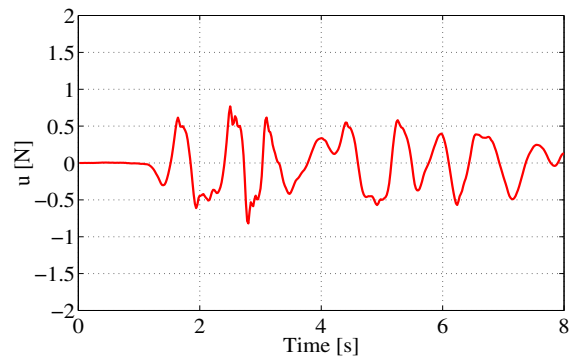
(c) u_s



(c) u_s



(d) u



(d) u

Fig. 16 Time history responses against Hanshin-Awaji earthquake (Level 2-2) by H_∞ fixed controller

Fig. 17 Time history responses against Hanshin-Awaji earthquake (Level 2-2) by SM controller

the maximum value of the first story acceleration by the SM controller becomes worse than that without control as shown in Figs. 14 (d) and (e).

Figures 15, 16 and 17 respectively show the experimental results of the GS controller, the H_∞ fixed controller and the SM controller against Hanshin-Awaji earthquake (Level 2-2). Figs 15, 16, 17 (a), (b), (c) and (d) respectively show the fourth story acceleration $\ddot{x}_4 + \ddot{z}$, the first story acceleration $\ddot{x}_1 + \ddot{z}$, the control input u_s and the controller output u . The dotted lines indicate responses without control. It is seen from Figs. 15 (a) and (b) that the GS controller holds reduction of the first story acceleration and the fourth story acceleration by 57 % and 32 %, respectively, at the maximum value even when actuator saturation occurs. From Figs. 16 and 17, it is seen that the H_∞ fixed controller and the SM controller remarkably lower the control performance by the actuator saturation. Especially, the first story acceleration response becomes worse than that without control at about 2.5 s. Furthermore, in case of the H_∞ fixed controller the spillover phenomenon due to truncated modes occurs by the actuator saturation.

CONCLUSIONS

In order to overcome actuator saturation problem in active vibration isolation of a multi-degree-of-freedom structure, we designed a gain-scheduled controller in accordance with a scheduling parameter considering the control input. The obtained gain-scheduled controller was compared with both an H_∞ fixed controller and an SM controller in simulations and experiments for a four-degree-of-freedom structure. As a result, it is verified that the GS controller was superior to other control methods in case of five representative earthquakes with which saturation phenomena of the actuator occur.

REFERENCES

1. Santo N, Yoshida K. "Sliding mode semi-active base isolation using the switching hyperplane designed by disturbance-accommodating bilinear control." Proceedings of the International Conference on Advances and New Challenges in Earthquake Engineering Research, Harbin, Hong Kong. 66, 2002.
2. Yoshida K. "First building with semi-active base isolation." Journal of the Japan Society of Mechanical Engineers 2001 (in Japanese); 104(995): 698-702.
3. Nishimura H, Kojima A. "Active vibration isolation control for a multi-degree-of-freedom structure with uncertain base dynamics." JSME International Journal Series C 1999; 41(1): 37- 45.
4. Nishimura H, Kojima A. "Seismic isolation control for a building-like structure." IEEE Control Systems Magazine 1999; 19(6): 38- 44.
5. Kim J-H, Jabbari F. "Actuator saturation and control design for buildings under seismic excitation." Journal of Engineering Mechanics 2002; 128(4): 403-412.
6. Nguyen T, Jabbari F, Miguel de S. "Controller designs for seismic-excited buildings with bounded actuator." Journal of Engineering Mechanics 1998; 124(8): 857-865.
7. Santo N, Watanabe T, Yoshida K. "Sliding mode control of base isolation system." Proceedings of the 2nd Japan-Korea Symposium of Frontiers in Vibration Science and Technology, Tokyo, Japan. 104-105, 1999.

8. Santo N, Ogaki H, Watanabe T, Yoshida K. "Active vibration isolation system using sliding mode controller." Proceedings of the D&D conference 2000 (in Japanese), Tokyo, Japan. No. 00-6, 130.pdf, 2000.
9. Nishimura H, Oie N. "Vibration control of a multi-degree-of-freedom structure taking account of actuator constraints." Proceedings of the 5th International Conference on Motion and Vibration Control, Sydney, Australia. Vol. 1, 239-244, 2000.
10. Shimodaira S, Nishimura H. "Active vibration isolation control for a structure taking account of actuator constraints." Proceedings of the 6th International Conference on Motion and Vibration Control, Saitama, Japan. Vol. 1, 70-75, 2002.
11. Gahinet P, Nemirovski A, Laub AJ, Chilali M. "LMI control toolbox, for use with MATLAB." Natick: Math Works Inc., 1995.
12. Takagi K, Nishimura H. "Gain-scheduled control of a tower crane considering varying load-rope length." JSME International Journal Series C 1999; 42(4): 914-921.
13. Itagaki N, Nishimura H, Takagi K. "Design method of gain-scheduled control system considering actuator saturation (Experimental verification for cart and inverted pendulum system)." JSME International Journal Series C 2003; 46(3): 953-959.